All-Inorganic Near-Infrared Luminescent Colloidal Silicon Nanocrystals: High Dispersibility in Polar Liquid by Phosphorus and Boron Codoping

ARTICLE *in* THE JOURNAL OF PHYSICAL CHEMISTRY C · AUGUST 2012

Impact Factor: 4.77 · DOI: 10.1021/jp305832x

THE JOURNAL OF PHYSICAL CHEMISTRY C

Article

pubs.acs.org/JPCC

All-Inorganic Near-Infrared Luminescent Colloidal Silicon Nanocrystals: High Dispersibility in Polar Liquid by Phosphorus and Boron Codoping

Hiroshi Sugimoto,[†] Minoru Fujii,*[,†] Kenji Imakita,[†] Shinji Hayashi,[†] and Kensuke Akamatsu[‡]

[†]Department of Electrical and Electronic Engineering, Graduate School of Engineering, Kobe University, Rokkodai, Nada, Kobe 657-8501, Japan

[‡]Department of Nanobiochemistry, Frontiers of Innovative Research in Science and Technology (FIRST), Konan University, 7-1-20 minatojimaminami, Chuo-ku, Kobe 650-0047, Japan

ABSTRACT: We demonstrate the formation of a new type of surfactant-free colloidal silicon nanocrystal (Si-NC). The characteristic structural feature of the Si-NCs is simultaneous doping of phosphorus (P) and boron (B) in and on the surface of Si-NCs. The codoped Si-NCs are stable in methanol for more than a year and exhibit luminescence in the near-infrared range. We perform comprehensive studies on the structure of codoped colloidal Si-NCs and discuss the mechanism of the high solution dispersibility.

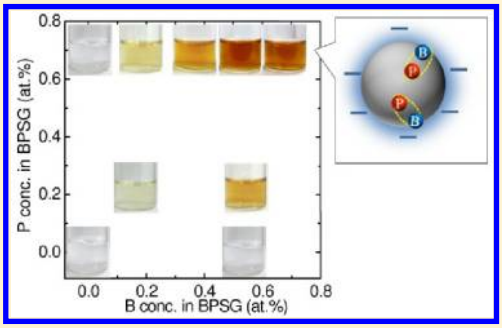

INTRODUCTION

Colloidal semiconductor nanocrystals (NCs) have been attracting considerable research attention because of the strong demands for the fabrication of large-area optoelectronic devices by vacuum-free printable processes. Two- and three-dimensional arrays of NCs (NC solids) are produced from colloids, and thin film transistors,[1,2] solar cells,[3,4] and light-emitting diodes[5,6] are fabricated. Among different kinds of semiconductor NCs, silicon (Si) NCs are the most important for some applications because of the nontoxicity, biocompatibility, natural abundance, and high compatibility to complementary metal oxide semiconductor (CMOS) device processes. The quality of colloidal Si-NCs has been improved significantly in the last several years, and those with high crystallinity, small size distribution, high stability in solution, and high luminescence quantum efficiency have been developed.[7−14]

One of the criteria of the quality of colloidal NCs is the long-term stability in solution. A commonly employed strategy to attain high stability is the functionalization of the NC surface with organic molecules. The surface molecules prevent agglomeration of NCs by electrostatic repulsion and steric barriers. However, the molecules sometimes exert fatal effects on NC solids because they act as tunneling barriers between NCs and degrade the conductivity.[15] To circumvent this problem, molecules that do not degrade the conductivity significantly, but still prevent agglomeration of NCs, have been explored.[16,17] Furthermore, additional processes to remove surfactants during or after film formation have been developed.[18,19] However, the postprocesses may induce defects on the surface of NCs and modify the electrical and optical properties. Therefore, development of surfactant-free stable colloidal Si-NCs is a very important research subject.

Recently, we have succeeded in producing colloidal Si-NCs without any surface functionalization processes.[20] The characteristic structural feature of the Si-NCs is simultaneous doping of phosphorus (P) and boron (B) in Si-NCs. P and B codoped colloidal Si-NCs are stable in polar liquids, and no precipitates are formed for more than a year without any special care during storage. Codoped colloidal Si-NCs exhibit bright PL in the near-infrared (NIR) range with the lifetime of several hundreds of microseconds.[20] These features of codoped Si-NCs are very attractive for applications in optoelectronic devices and biology. However, the structure of codoped Si-NCs is not fully analyzed and the origin of the high solution dispersibility is not clarified. Furthermore, the role of two kinds of impurity atoms on the solution dispersibility is not known.

In this work, we perform comprehensive studies on the codoped Si-NCs to clarify the structure and the mechanism of the solution dispersibility. By changing impurity concentrations in the preparation processes in wide ranges, we study the role of impurity atoms in the solution dispersibility and propose a structural model of codoped colloidal Si-NCs.

EXPERIMENTAL SECTION

P and B codoped colloidal Si-NCs are prepared by a previously reported procedure.[20] Borophosphosilicate glass (BPSG) films containing P and B codoped Si-NCs were first prepared on thin

Received: June 14, 2012
Revised: July 30, 2012
Published: July 30, 2012

   dx.doi.org/10.1021/jp305832x | J. Phys. Chem. C 2012, 116, 17969−17974

stainless steel plates by cosputtering Si, SiO_2, B_2O_3, and P_2O_5.[20−23] The Si-rich BPSG films were then peeled from the plates and annealed in a N_2 gas atmosphere at 1150 °C for 30 min to grow Si-NCs in BPSG matrixes.[20,24] During the growth, impurity atoms are incorporated into Si-NCs.[20−23] To isolate Si-NCs from BPSG matrixes, the films were dissolved in hydrofluoric acid (HF) solution (46 wt %) for 1 h in an ultrasonic bath. This process results in the preparation of HF solution containing isolated Si-NCs. Isolated Si-NCs were separated from the HF solution by centrifugation (4000 rpm, 1 min) in an ultrafiltration concentrator (VS0232: Sartorius Stedim Biotech GmbH), and Si-NC powder was obtained in the concentrator. Methanol was then added to the concentrator to disperse Si-NCs in methanol. The same procedure was repeated several times to remove HF.

As we will show later, for the samples within specific P and B concentration ranges, a majority of Si-NCs are dispersed in methanol. On the other hand, in some samples, a fraction of Si-NCs are precipitated. The precipitates were removed by centrifugation (4000 rpm, 1 min), and a supernatant liquid was collected. The clear liquids were kept in a vial at room temperature. All the processes were performed in air, and a glovebox was not necessary for the preparation (see Figure 1).

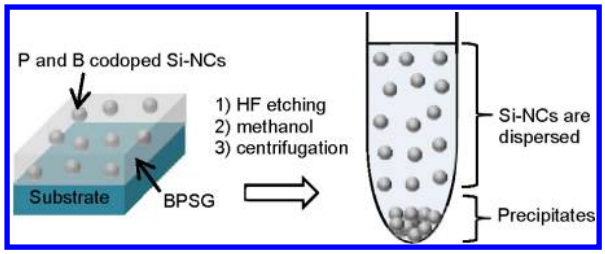

Figure 1. Schematic illustration of the preparation procedure of P and B codoped colloidal Si-NCs. Codoped Si-NCs embedded in BPSG thin films prepared by a cosputtering method are dissolved in HF solutions. Isolated Si-NCs are dispersed in methanol. Precipitates are removed by centrifugation, and a clear solution is obtained.

RESULT AND DISCUSSION

Codoped Si-NCs in solutions were characterized by transmission electron microscopy (TEM) (JEOL JEM-200CX). For TEM observations, the solution containing Si-NCs was dropped on carbon-coated copper grids. Figure 2a shows a typical TEM image of Si-NCs dispersed in methanol. We can see that particles about 3 nm in diameter (black spots) are densely packed. It is interesting to note that only a monolayer of particles is formed, and no three-dimensional agglomerates are observed. The inset of Figure 2a shows the electron diffraction pattern of the particles. The diffraction rings agree well with that of a Si crystal with the diamond structure (JCPDS No. 27-1402). Figure 2b is a high-resolution TEM (HRTEM) image of one of the particles. Lattice fringes corresponding to the {111} planes of a Si crystal can be seen. The Si-NC is a defect-free single crystal, and amorphous or oxide shells are not clearly observed. We observed a large number of Si-NCs by HRTEM and found that almost all of them are defect-free single crystals. Figure 2c shows the size distribution of Si-NCs dispersed in the solution obtained from TEM images. The average diameter is 3.0 nm with the standard deviation of 0.9 nm.

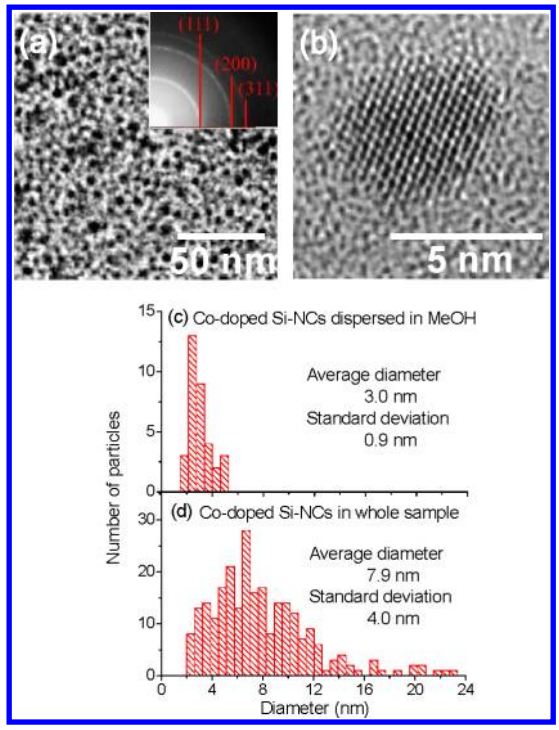

Figure 2. (a) Bright-field TEM image of P and B codoped colloidal Si-NCs on a carbon-coated Cu mesh. The inset is the electron diffraction pattern. (b) HRTEM image of a P and B codoped Si-NC. The lattice fringes correspond to {111} planes of Si. The background amorphous image is from a carbon thin film. The size distribution of (c) codoped Si-NCs dispersed in methanol and (d) those in a whole sample containing precipitates.

To investigate the difference between NCs dispersed in solution and precipitated in the bottom of a vial, we observe a whole sample containing agglomerates, that is, a solution before removing precipitates, by TEM. Figure 2d shows the size distribution obtained from TEM images. The size distribution is much broader than that of Si-NCs dispersed in solution. In Figure 2d, the average diameter is 7.9 nm and the standard deviation is 4.0 nm. The comparison between panels c and d in Figure 2 indicates that, within a large size distribution, only Si-NCs smaller than 6 nm are dispersed in methanol. The size is thus an important parameter to attain high solution dispersibility for P and B codoped Si-NCs.

Figure 3 shows the infrared (IR) absorption spectrum of a KBr plate on which colloidal Si-NCs are drop-casted. In addition to the O−H vibration bands probably due to adsorbed water, those assigned to the Si−O−Si stretching (1080 cm^{-1}) and rocking (~480 cm^{-1}) modes and the B−O stretching mode (~1400 cm^{-1}) are observed. The surface of Si-NCs is thus slightly oxidized in methanol or by exposure in air,[25] although thick oxide layers are not formed, as confirmed by HRTEM observations. No peaks corresponding to C−H vibration modes (~2900 cm^{-1}) are observed in IR absorption spectra, confirming that the surface of codoped Si-NCs is not functionalized by organic molecules.

Figure 4 shows the photographs of colloidal Si-NCs prepared from Si-rich BPSG films with different P and B concentrations. The abscissa and ordinate of Figure 4 represent B and P concentrations, respectively, in as-deposited Si-rich BPSG films. The P concentration is determined by energy-dispersive X-ray spectroscopy (EDS),[26] and the B concentration is obtained

dx.doi.org/10.1021/jp305832x | J. Phys. Chem. C 2012, 116, 17969−17974

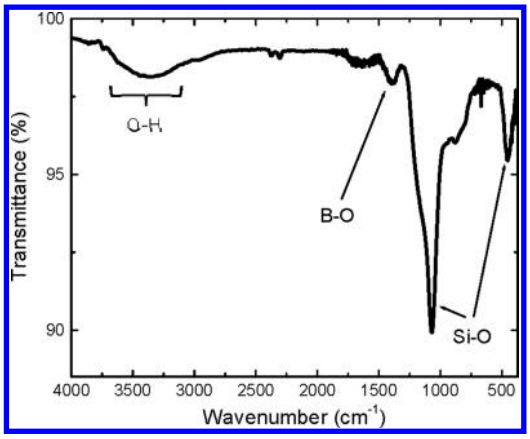

Figure 3. IR absorption spectrum of codoped colloidal Si-NCs.

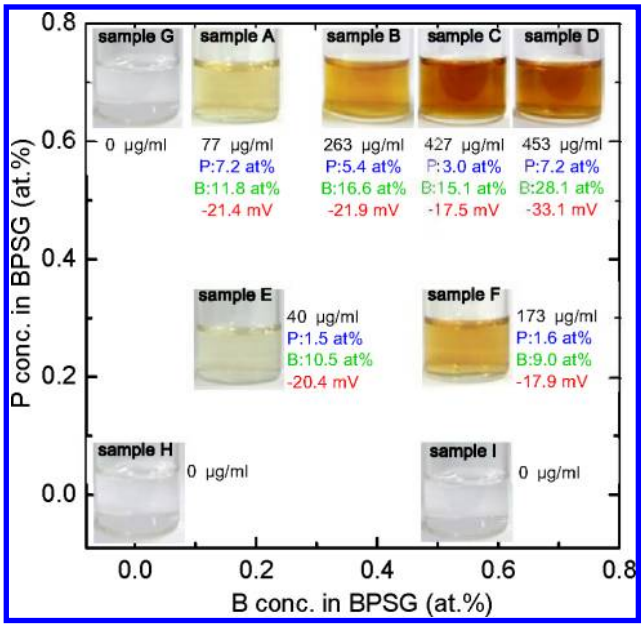

Figure 4. Photographs of the solutions after removing precipitates by centrifugation. The abscissa and ordinate are B and P concentrations, respectively, in as-deposited Si-rich BPSG films. The numbers below the pictures are the amounts of Si in the solution, P and B concentrations in Si-NCs, and the ζ-potentials.

from the intensity ratio of Si−O and B−O vibration modes in IR absorption spectra.[21−23,27] The photographs of the solutions after removing precipitates by centrifugation are shown. The color of the solution depends strongly on sample preparation parameters. Note that the amount of Si-NC-doped BPSG films dissolved in HF is the same for all the samples. Therefore, a dense color implies that a large fraction of Si-NCs are dispersed in solution. On the other hand, a light color means that a majority of Si-NCs are precipitated and removed by centrifugation. Below the photographs in Figure 4, the amounts of Si-NCs in the solutions obtained by inductively coupled plasma atomic emission spectrometry (ICP-AES) measurements are shown. In undoped Si-NCs (sample H), the solution is colorless and Si is not detected in ICP-AES. Therefore, undoped Si-NCs are not dispersed in polar liquids. This is consistent with previous reports.[8,11,28] Similarly, in P (sample G) and B (sample I) singly doped samples, Si is not detected in ICP-AES and the solutions are colorless. In contrast to these samples, P and B codoped samples (samples A−F) are brownish. The color becomes dense and the amount of Si in solution increases with increasing P and B concentrations. In the darkest solution (sample D), the Si concentration is 453 μg/mL. It should be stressed here that, even in the darkest solution, optical transmittance in the transparent wavelength of the Si crystal is larger than 95%, and thus, the dense color is not due to light scattering, but absorption. Figure 4 clearly demonstrates that codoping of P and B is essential to achieving high solution dispersibility.

In Figure 4, P and B concentrations in colloidal Si-NCs obtained by ICP-AES measurements are also shown below the photographs. We can see that the P and B concentrations, especially the B concentrations, are very high. They are much higher than those in Si-rich BPSG films before etching (see abscissa and ordinate in Figure 4). The difference in the P and B concentrations between Si-NCs in solution and Si-rich BPSG films before etching indicates that P and B atoms are accumulated in or on the surface of Si-NCs during the growth of Si-NCs by annealing. The P and B concentrations in colloidal Si-NCs are also much higher than the solid solubility limits of P and B in the bulk Si crystal.[29] Doping of such a high amount of impurities in substitutional sites of Si-NCs is energetically not favorable.[30,31] Therefore, a majority of impurity atoms are considered to be accumulated on the surface of Si-NCs, and only a fraction of them are doped in the substitutional sites.

To confirm that B and P are simultaneously doped in all Si-NCs, we compare *Z*-contrast high-angle annular dark-field (HAADF) images and electron energy loss spectroscopy (EELS) mappings by scanning TEM (Hitachi, HD2700). Figure 5a shows a HAADF image of sample C. White spots are

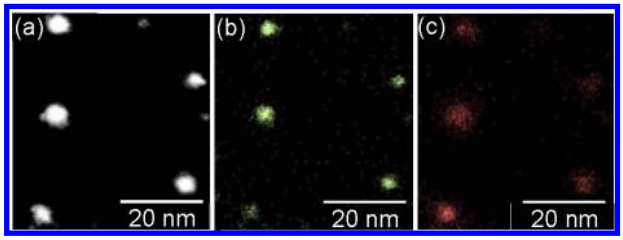

Figure 5. (a) HAADF STEM image of codoped Si-NCs. EELS mapping of (b) P and (c) B. All images are taken at the same position.

Si-NCs. Figure 5b,c shows EELS mapping images of P and B in the same region. We can see that the three images coincide perfectly. The perfect coincidence can be seen in all particles. This confirms that very high P and B concentrations in solutions obtained by ICP-AES measurements are not due to the formation of B and P clusters in solutions but are due to simultaneous doping of very large amounts of B and P in or on the surface of Si-NCs.

In Figure 4, ζ-potentials of the solutions are also shown. The ζ-potentials are around −20 mV for samples A−C, E, and F, and around −30 mV for sample D. The surface of codoped Si-NCs is thus negatively charged, and the electrostatic repulsion between Si-NCs is the origin of the high dispersibility in methanol. The similar values of the ζ-potentials in samples A−C, E, and F suggest that the surface structure of Si-NCs dispersible in solution is similar, irrespective of the P and B concentrations in Si-rich BPSG films before etching, and only the amount of Si-NCs satisfying a specific condition for high solution dispersibility is different depending on preparation parameters. The reason that sample D has about a 50% larger ζ-

dx.doi.org/10.1021/jp305832x | J. Phys. Chem. C 2012, 116, 17969−17974

potential than others is not clear, but probably this is related to an extremely high B concentration in sample D.

Figure 6a shows normalized PL spectra of codoped colloidal Si-NCs. The excitation wavelength is 405 nm. As reported in

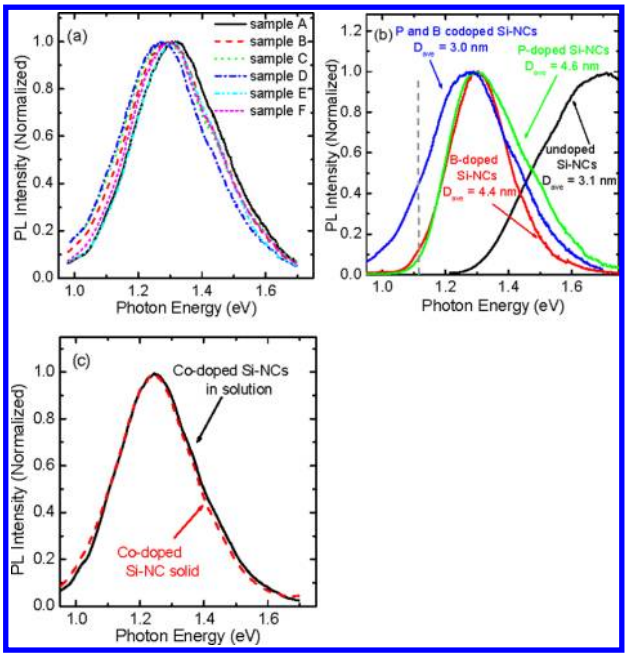

Figure 6. (a) Normalized PL spectra of samples A–F. (b) Normalized PL spectra of undoped, P-doped, B-doped, and P and B codoped Si-NCs in methanol. (c) Normalized PL spectra of colloidal codoped Si-NCs in methanol and NC solids prepared by drop-casting the colloid.

our previous work, the PL spectrum of codoped colloidal Si-NCs shifts to higher energy by keeping them in methanol and is almost stabilized in a month.[20] Therefore, the spectra in Figure 6a are measured about 1 month after preparation. The codoped colloidal Si-NCs exhibit a broad PL with the maximum around 1.3 eV. The PL maximum depends slightly on samples, but the difference is very small. The very small dependence of the PL energy on the sample preparation condition is different from that observed for codoped Si-NCs in BPSG films before etching. In that case, the PL spectra depend strongly on the preparation parameters.[21−23]

Figure 6b compares PL spectra of undoped, P or B singly doped, and P and B codoped Si-NCs in methanol. As described above, undoped and P or B singly doped Si-NCs are not dispersed in methanol and precipitate in the bottom of a vial. Therefore, the solutions are continuously stirred by a magnetic stirrer during measurements. Note that the PL intensities of P or B singly doped Si-NCs are much smaller than those of intrinsic and codoped Si-NCs.[21−23,32] The PL peak energy of codoped Si-NCs is much lower than that of undoped Si-NCs, although the diameters are similar. This suggests that impurity states are involved in the optical transitions in codoped Si-NCs. In our previous work,[21−23] we studied the PL properties of doped Si-NCs in detail and assigned the low-energy PL of codoped Si-NCs to the transitions between donor and acceptor states. The PL properties of codoped Si-NCs are also different from those of B or P singly doped Si-NCs in some aspects, that is, the lifetime, the intensity, and the spectral shape, although we do not discuss them in this paper.[21−23,32−34]

Figure 6c shows the PL spectrum of a Si-NC solid prepared by drop-casting colloidal Si-NCs on a quartz substrate and drying in air. For the comparison, the spectrum of colloidal Si-NCs in methanol is also shown. There is no difference between the spectra of the solution and the solid. This indicates that codoped colloidal Si-NCs are very stable in air exposure. This is the advantage of the present codoped colloidal Si-NCs compared to surface-functionalized NCs, because they are sometimes very vulnerable to air exposure.[35,36]

From these experimental results, we discuss the structure and the origin of the negative surface potentials of codoped colloidal Si-NCs. As clearly shown in Figure 4, the existence of either P or B is not a sufficient condition for the high dispersibility, and the simultaneous doping of P and B is the necessary condition. The problem is whether P and B are randomly distributed in or on the surface of Si-NCs or they form P–B pairs. Ossicini et al. showed by first-principles calculations that the formation energy of P and B codoped Si-NCs is much smaller than those of either P or B singly doped Si-NCs.[37−40] Furthermore, the formation energy is the smallest when P and B atoms are in the nearest neighbor and when the pair is located near the surface.[37−40] Therefore, in the present work, at least part of P and B atoms are considered to be doped in the subsurface of Si-NCs as pairs.

In Figure 7, the models of undoped, P or B singly doped, and P and B codoped Si-NCs are shown. The surface of undoped

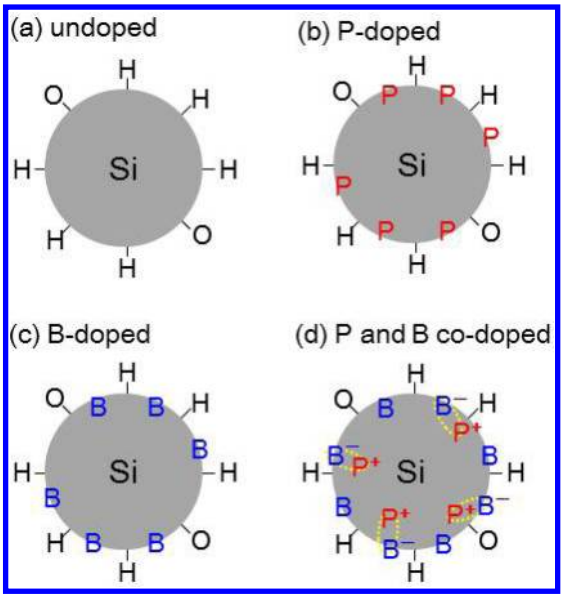

Figure 7. Proposed structural models of (a) undoped, (b) P-doped, (c) B-doped, and (d) P and B codoped Si-NCs in solution.

Si-NCs is terminated by O and H (Figure 7a). In P or B singly doped Si-NCs, electrically active impurities are considered to be doped in the subsurface,[24,41−43] and inactive impurities are considered to be accumulated on the surface. These surface impurities do not contribute to the solution dispersibility of Si-NCs, as shown in Figure 4. Figure 7d shows a structural model of codoped Si-NCs. The specific structural feature of codoped Si-NCs is the existence of P–B pairs. Since the B concentration is always larger than the P concentration in codoped Si-NCs (see Figure 4), the maximum number of P–B pairs may be determined by the P concentration, and excess B may exist on the surface of Si-NCs.

If the proposed structural model is correct, what is the origin of the negative surface potential? A possible model is that there

dx.doi.org/10.1021/jp305832x | J. Phys. Chem. C 2012, 116, 17969–17974

is a specific alignment of P−B pairs in the radial direction of Si-NCs. If ionized B atoms (B^-) are located on the surface side and ionized P atoms (P^+) are on the core side, a negative potential will be induced on the surface. Detailed theoretical studies on the preferable sites of P−B pairs in codoped Si-NCs are indispensable to prove the model.

Another possible explanation of the high solution dispersibility is the formation of specific types of borate and/or phosphate that are not dissolved in HF solution on the surface of Si-NCs, although the formation of such structures is not shown within the present work. Further detailed analytical research is necessary to fully elucidate the surface structure.

Finally, we demonstrate that codoped Si-NCs can be dispersed in water. Figure 8a shows the optical transmittance

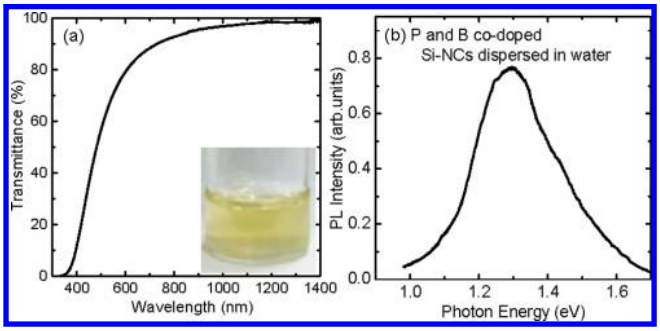

Figure 8. (a) Optical transmittance spectrum of codoped Si-NCs in water. The inset is the photograph of the solution. (b) PL spectrum of codoped Si-NCs dispersed in water.

spectrum of codoped colloidal Si-NCs in distilled water. The inset is the photograph of the solution. The transmittance in the transparent range is almost 100%, and thus, light scattering is negligibly small. No agglomerates were observed in TEM. Therefore, codoped Si-NCs can also be dispersed in water. Figure 8b shows the PL spectrum of codoped colloidal Si-NCs in water. The PL peak is around 1.3 eV. The spectrum is almost identical to those in methanol. Since the PL energy is in the transparent window of biological cells, the codoped Si-NCs may be useful as phosphors in bioimaging.

CONCLUSION

We performed comprehensive studies on P and B codoped colloidal Si-NCs and revealed the conditions to achieve high dispersibility in polar liquids. We found that simultaneous doping of P and B is an essential condition for the high dispersibility. Furthermore, we showed that only Si-NCs smaller than 6 nm in diameter are dispersed in solution. From the characterization of the codoped colloidal Si-NCs, we proposed a model where pairs of P and B in the subsurface of Si-NCs play a crucial role for inducing a negative surface potential in Si-NCs, and the surface potential is the origin of the high dispersibility. The codoped colloidal Si-NCs showed a PL around 1.3 eV. The PL properties of Si-NC solids prepared from the colloids were very similar to those of the colloids, and the PL was very stable in air.

AUTHOR INFORMATION

Corresponding Author

*E-mail: fujii@eedept.kobe-u.ac.jp.

Notes

The authors declare no competing financial interest.

ACKNOWLEDGMENTS

The authors thank Mr. M. Fukuda for valuable discussions. This work is supported, in part, by KAKENHI (23310077, 24651143).

REFERENCES

(1) Talapin, D.; Murray, C. *Science* **2005**, *310*, 86−89.
(2) Urban, J.; Talapin, D.; Shevchenko, E.; Kagan, C.; Murray, C. *Nat. Mater.* **2007**, *6*, 115−121.
(3) Gur, I.; Fromer, N.; Geier, M.; Alivisatos, A. *Science* **2005**, *310*, 462−465.
(4) Mcdonald, S.; Konstantatos, G.; Zhang, S.; Cyr, P.; Klem, E.; Levina, L.; Sargent, E. *Nat. Mater.* **2005**, *4*, 138−142.
(5) Tan, Z.; Zhang, F.; Zhu, T.; Xu, J.; Wang, A.; Dixon, J.; Li, L.; Zhang, Q.; Mohney, S.; Ruzyllo, J. *Nano Lett.* **2007**, *7*, 3803−3807.
(6) Cheng, K.; Anthony, R.; Kortshagen, U.; Holmes, R. *Nano Lett.* **2010**, *10*, 1154−1157.
(7) Erogbogbo, F.; Yong, K.; Roy, I.; Xu, G.; Prasad, P.; Swihart, M. *ACS Nano* **2008**, *2*, 873−878.
(8) Gupta, A.; Swihart, M.; Wiggers, H. *Adv. Funct. Mater.* **2009**, *19*, 696−703.
(9) Mangolini, L.; Kortshagen, U. *Adv. Mater.* **2007**, *19*, 2513−2519.
(10) Pettigrew, K.; Liu, Q.; Philip, P.; Kauzlarich, S. *Chem. Mater.* **2003**, *15*, 4005−4011.
(11) Sato, S.; Swihart, M. *Chem. Mater.* **2006**, *18*, 4083−4088.
(12) Mastronardi, M. L.; Maier-Flaig, F.; Faulkner, D.; Henderson, E. J.; Kübel, C.; Lemmer, U.; Ozin, G. A. *Nano Lett.* **2012**, *12*, 337−342.
(13) Beard, M.; Knutsen, K.; Yu, P.; Luther, J.; Song, Q.; Metzger, W.; Ellingson, R.; Nozik, A. *Nano Lett.* **2007**, *7*, 2506−2512.
(14) Hessel, C.; Reid, D.; Panthani, M.; Rasch, M.; Goodfellow, B.; Wei, J.; Fujii, H.; Akhavan, V.; Korgel, B. *Chem. Mater.* **2012**, *24*, 393−401.
(15) Liu, Y.; Gibbs, M.; Puthussery, J.; Gaik, S.; Ihly, R.; Hillhouse, H.; Law, M. *Nano Lett.* **2010**, *10*, 1960−1969.
(16) Nag, A.; Kovalenko, M. V.; Lee, J.-S.; Liu, W.; Spokoyny, B.; Talapin, D. V. *J. Am. Chem. Soc.* **2011**, *133*, 10612−10620.
(17) Fafarman, A. T.; Koh, W.-K.; Diroll, B. T.; Kim, D. K.; Ko, D.-K.; Oh, S.-J.; Ye, X.; Doan-Nguyen, V.; Crump, M. R.; Reifsnyder, D. C.; et al. *J. Am. Chem. Soc.* **2011**, *133*, 15753−15761.
(18) Wills, A. W.; Kang, M. S.; Khare, A.; Gladfelter, W. L.; Norris, D. J. *ACS Nano* **2010**, *4*, 4523−4530.
(19) Zhang, H.; Hu, B.; Sun, L.; Hovden, R.; Wise, F.; Muller, D.; Robinson, R. *Nano Lett.* **2011**, *11*, 5356−5361.
(20) Fukuda, M.; Fujii, M.; Sugimoto, H.; Imakita, K.; Hayashi, S. *Opt. Lett.* **2011**, *36*, 4026−4028.
(21) Fujii, M.; Toshikiyo, K.; Takase, Y.; Yamaguchi, Y.; Hayashi, S. *J. Appl. Phys.* **2003**, *94*, 1990−1995.
(22) Fujii, M.; Yamaguchi, Y.; Takase, Y.; Ninomiya, K.; Hayashi, S. *Appl. Phys. Lett.* **2004**, *85*, 1158−1160.
(23) Fujii, M.; Yamaguchi, Y.; Takase, Y.; Ninomiya, K.; Hayashi, S. *Appl. Phys. Lett.* **2005**, *87*, 211919.
(24) Sugimoto, H.; Fujii, M.; Fukuda, M.; Imakita, K.; Hayashi, S. *J. Appl. Phys.* **2011**, *110*, 063528.
(25) Lin, S.; Chen, D. *Small* **2009**, *5*, 72−76.
(26) Ito, M.; Imakita, K.; Fujii, M.; Hayashi, S. *J. Phys. D: Appl. Phys.* **2010**, *43*, 505101.
(27) Tenney, A. *J. Electrochem. Soc.* **1971**, *118*, 1658−1661.
(28) Hua, F.; Swihart, M.; Ruckenstein, E. *Langmuir* **2005**, *21*, 6054−6062.
(29) Sze, S. M. *Physics of Semiconductor Devices*, 2nd ed.; Wiley: New York, 1981.
(30) Dalpian, G.; Chelikowsky, J. *Phys. Rev. Lett.* **2006**, *96*, 226802−226805.
(31) Iori, F.; Ossicini, S.; Degoli, E.; Luppi, E.; Poli, R.; Magri, R.; Cantele, G.; Trani, F.; Ninno, D. *Phys. Status Solidi A* **2007**, *204*, 1312−1317.
(32) Fujii, M.; Hayashi, S.; Yamamoto, K. *J. Appl. Phys.* **1998**, *83*, 7953−7957.

(33) Fujii, M.; Mimura, A.; Hayashi, S.; Yamamoto, K. *Appl. Phys. Lett.* **1999**, *75*, 184−186.
(34) Mimura, A.; Fujii, M.; Hayashi, S.; Kovalev, D.; Koch, F. *Phys. Rev. B* **2000**, *62*, 12625−12627.
(35) Sykora, M.; Koposov, A. Y.; McGuire, J. A.; Schulze, R. K.; Tretiak, O.; Pietryga, J. M.; Klimov, V. I. *ACS Nano* **2010**, *4*, 2021−2034.
(36) Chappell, H.; Hughes, B.; Beard, M.; Nozik, A.; Johnson, J. *J. Phys. Chem. Lett.* **2011**, *2*, 889−893.
(37) Iori, F.; Degoli, E.; Magri, R.; Marri, I.; Cantele, G.; Ninno, D.; Trani, F.; Pulci, O.; Ossicini, S. *Phys. Rev. B* **2007**, *76*, 085302.
(38) Ossicini, S.; Degoli, E.; Iori, F.; Luppi, E.; Magri, R.; Cantele, G.; Trani, F.; Ninno, D. *Appl. Phys. Lett.* **2005**, *87*, 173120.
(39) Cantele, G.; Degoli, E.; Luppi, E.; Magri, R.; Ninno, D.; Iadonisi, G.; Ossicini, S. *Phys. Rev. B* **2005**, *72*, 113303.
(40) Iori, F.; Ossicini, S. *Physica E* **2009**, *41*, 939−46.
(41) Pii, X.; Gresback, R.; Liptak, R.; Campbell, S.; Kortshagen, U. *Appl. Phys. Lett.* **2008**, *92*, 123102.
(42) Melnikov, D. V.; Chelikowsky, J. R. *Phys. Rev. Lett.* **2004**, *92*, 046802.
(43) Baldwin, R. K.; Zou, J.; Pettigrew, K. A.; Yeagle, G. J.; Britt, R. D.; Kauzlarich, S. M. *Chem. Commun.* **2006**, 658−660.